

## Fabry-Perot Interferometer with Quantum Mirrors: Nonlinear Light Transport and Rectification

F. Fratini,<sup>1,2,3,4,\*</sup> E. Mascarenhas,<sup>1</sup> L. Safari,<sup>4,5</sup> J-Ph. Poizat,<sup>2,3</sup> D. Valente,<sup>6</sup>  
A. Auffèves,<sup>2,3</sup> D. Gerace,<sup>7</sup> and M. F. Santos<sup>1</sup>

<sup>1</sup>*Departamento de Física, Universidade Federal de Minas Gerais, CP 702, 30123-970 Belo Horizonte, Brazil*

<sup>2</sup>*Université Grenoble Alpes, Institut NÉEL, F-38042 Grenoble, France*

<sup>3</sup>*CNRS, Institut NÉEL, F-38042 Grenoble, France*

<sup>4</sup>*Department of Physics, University of Oulu, Box 3000, FI-90014 Oulu, Finland*

<sup>5</sup>*IST Austria, Am Campus 1, A-3400 Klosterneuburg, Austria*

<sup>6</sup>*Instituto de Física, Universidade Federal de Mato Grosso, 78060-900 Cuiabá MT, Brazil*

<sup>7</sup>*Dipartimento di Fisica, Università di Pavia, via Bassi 6, I-27100 Pavia, Italy*

(Received 6 June 2014; published 8 December 2014)

Optical transport represents a natural route towards fast communications, and it is currently used in large scale data transfer. The progressive miniaturization of devices for information processing calls for the microscopic tailoring of light transport and confinement at length scales appropriate for upcoming technologies. With this goal in mind, we present a theoretical analysis of a one-dimensional Fabry-Perot interferometer built with two highly saturable nonlinear mirrors: a pair of two-level systems. Our approach captures nonlinear and nonreciprocal effects of light transport that were not reported previously. Remarkably, we show that such an elementary device can operate as a microscopic integrated optical rectifier.

DOI: [10.1103/PhysRevLett.113.243601](https://doi.org/10.1103/PhysRevLett.113.243601)

PACS numbers: 42.50.Nn, 42.50.St, 42.60.Da, 42.65.-k

*Introduction.*—There is a growing interest in the realization of quantum optical systems in which single emitters are strongly coupled to one-dimensional (1D) radiation modes for efficient light transport [1–3] and quantum information processing [4]. The ultimate goal would be to progressively replace or hybridize current microelectronics with integrated optical devices in order to enhance data capacity, transmission velocity, and efficiency. One of the benchmarks for information processing is the ability to control the directionality of energy flux within a specific system architecture, a task that generically requires 1D propagation channels and nonlinear components. Furthermore, so-called rectifying devices provide the unidirectional isolation of strategic centers in electronic circuits. The combination of these properties has allowed for the technological revolution of microelectronic processors in the last century, and a similar development for the transport of light is necessary if one is to expect photon-based computing systems. In this Letter, we show how two-level quantum systems may be employed as nonlinear mirrors forming a Fabry-Perot (FP) interferometer. Optical rectification is a direct consequence of the nonlinear nature of such an interferometer. If integrated within an optical circuit, this rectifying device would prevent unwanted signals (or noise) to travel back, thus preserving the processing capabilities at the source. This is of utmost importance in the quantum regime, e.g., to prevent decoherence at the sender of the signals.

Several experiments have already demonstrated the combination of strong nonlinear behavior and 1D light propagation in different system implementations, such as trapped ions coupled to focused light beams or optical fibers [5,6],

superconducting circuits coupled to microwave transmission lines [7–9], and semiconductor quantum dots or vacancy (e.g., nitrogen vacancy) centers coupled to photonic or plasmonic waveguides [10–13]. Among these attempts, the use of solid state quantum emitters as artificial two-level systems (TLSs) is specially promising due to their nanoscale dimensions, their extreme nonlinear properties, and their tunability, thanks to the use of external electrostatic gates [14], applied magnetic fields [15,16], or mechanical strain [10]. These combined advantages have led to a wide range of theoretical proposals and recent experiments, with the aim of building single photon emitters [17], single-photon light switches and transistors [2], quantum optical diodes [18–20], and interferometers [21]. Following these proposals, a pair of TLSs coupled to a 1D waveguide can be expected as one of the simplest configurations where tunable nonlinear and nonreciprocal optical phenomena at the quantum level could be practically realized, besides allowing for photonic mediated interactions between distant qubits [22–24].

In this work we employ a semiclassical analysis to theoretically treat the transport of light in a quantum Fabry-Perot (QFP) interferometer built from two TLSs embedded in a 1D photonic channel, drawing inspiration from the recently demonstrated analogy between a single TLS and an optical mirror [5]. After validating our theoretical approach through comparison with previous results based on a similar model for the case of two identical TLSs [1,9,24], we thoroughly study the case of two different TLSs. In this latter case, we show that the QFP interferometer manifests nonreciprocal effects, not captured in

previous works, that enable us to rectify light transport through the 1D channel. Remarkably, we find regions where both light rectification and transmission exceed 92%, depending on the system parameters. In our approach, the TLSs are treated as quantum systems, and rectification emerges out of their highly nonlinear behavior, while the light field is treated as a classical input. Given the generality of this method in describing light transport within this QFP interferometer, our results can be adapted to a number of different physical implementations, as discussed at the end of the Letter. Differently from previous proposals [19,25–27], our QFP interferometer does not require the application of external fields to produce nonlinear effects on light transport.

*Fabry-Perot model.*—We consider two TLSs embedded in a 1D waveguide, as shown in Fig. 1. Light with angular frequency  $\omega$  and power  $p_{\text{inc}}$  is injected into the waveguide. We shall use the terms “intensity” and “power” interchangeably throughout the Letter. For these, we will use the symbol  $p$ , which is a dimensionless quantity representing the number of photons per lifetime. We denote with TLS1 (TLS2) the first (second) quantum emitter lying on the light path, if light is shined from left to right as in Fig. 1. The TLS1 (TLS2) has transition frequency  $\omega_{1(2)}$ , decay rate  $\gamma_{1(2)}$ , and position  $z = 0$  ( $z = L$ ). The detuning of the incoming light with respect to the TLS1 (TLS2) transition frequency is  $\delta\omega_1 = \omega - \omega_1$  ( $\delta\omega_2 = \omega - \omega_2$ ). Within a semiclassical approach, we treat such a system in analogy to a Fabry-Perot interferometer (see Fig. 1), where the reflectances of the mirrors are given by the reflectances of the TLSs, as obtained in a quantum mechanical framework. These latter can be readily derived from Ref. [28] (see Ref. [29]):

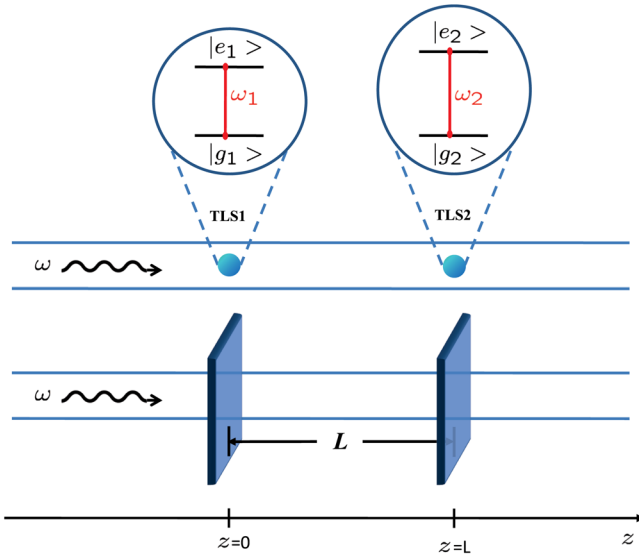


FIG. 1 (color online). A pair of two-level quantum systems in a one-dimensional waveguide as a quantum Fabry-Perot interferometer, and its classical counterpart.

$$R_{1(2)} = \frac{\gamma_{1(2)}^2}{\gamma_{1(2)}^2 + 4\delta\omega_{1(2)}^2 + 4p_{1(2)}\gamma_{1(2)}^2}, \quad (1)$$

where  $p_{1(2)}$  is the power impinging onto the TLS1 (TLS2); i.e.,  $\gamma_{1(2)}p_{1(2)}$  is the number of photons per second impinging onto the TLS1 (TLS2). The quantity  $R_{1(2)}$  represents the fraction of light power that the TLS1 (TLS2) reflects back into the 1D channel. Furthermore,  $\theta_{1(2)} = \arctan[2\delta\omega_{1(2)}/\gamma_{1(2)}]$  is the phase shift given by the TLS1 (TLS2) to the light upon reflection [24]. The phase shift given by either TLS to the transmitted light is neglected, as usual for mirrors.

The fraction of light power that the FP interferometer transmits, i.e., the FP transmittance, can be calculated as [29]

$$T = \frac{1}{F_1 + F_2 \sin^2(2\mu + \theta_+)}, \quad (2)$$

where

$$F_1 = \frac{(1 - \sqrt{R_1 R_2})^2}{(1 - R_1)(1 - R_2)}, \quad F_2 = \frac{4\sqrt{R_1 R_2}}{(1 - R_1)(1 - R_2)}, \quad (3)$$

while  $\mu = n\omega L/(2c)$ ,  $n$  is the effective refractive index of the waveguide,  $c$  is the speed of light in vacuum, and  $\theta_+ = (\theta_1 + \theta_2)/2$ . In order to use Eq. (2), we need first to find what the values for  $R_1$  and  $R_2$  are. This reduces to the question of finding what the values for  $p_1$  and  $p_2$  are. These latter can be obtained by numerically solving a system of coupled equations. The details of such a calculation are given in the Supplemental Material [29]. Thus, by using Eqs. (2) and (1), together with the numerical values for  $p_{1,2}$ , the transmittance  $T$  can be numerically calculated for any set of the (externally adjustable) variables  $\gamma_{1,2}$ ,  $\delta\omega_{1,2}$ ,  $L$ ,  $p_{\text{inc}}$ .

*Nonlinear light transport.*—The semiclassical approach employed in this work has been fully validated by comparing our results to solutions based on quantum mechanical models taken from the literature [1,9,24] (see Ref. [29]). In particular, we stress that the present approach allows us to calculate the light transport for any incident light power, as well as for different atomic frequencies and decay rates, in contrast to Refs. [1,24].

First, we explore the light intensity between the TLSs (intracavity intensity) and at the TLS positions, respectively. For simplicity, in the following we will consider  $\gamma_1 = \gamma_2 = 1 \equiv \gamma$  and  $L$  in units of the photon wavelength  $\lambda = 2\pi c/(n\omega)$ . In a standard FP interferometer, a large intracavity intensity is present when the mirror reflectances are close to 1. In line with our analogy, high intracavity intensity is expected in the present model when the TLS reflectances  $R_{1,2}$  are nearly 1, which is the case when light is shined in resonance with the TLSs and at low incident power. Let us denote by  $p_{\text{intr}}(z)$  the intracavity intensity at the position  $z$ , where  $0 < z < L$ , and by  $\langle p_{\text{intr}}(z) \rangle$  the average intracavity intensity:  $\langle p_{\text{intr}}(z) \rangle = \int_0^L p_{\text{intr}}(z) dz/L$ .

In Figs. 2(a) and 2(b), these two quantities are plotted as a function of  $p_{\text{inc}}$  and  $z$ , respectively. From Fig. 2(a) we notice that the relation between  $\langle p_{\text{intr}}(z) \rangle$  and  $p_{\text{inc}}$  is nonlinear. In fact, by supposing low incident power and  $\delta\omega_1 = \delta\omega_2 = 0$ , it can be analytically shown that the average intracavity intensity is well approximated by  $\langle p_{\text{intr}}(z) \rangle \approx \sqrt{p_{\text{inc}}}$ . In Fig. 2(a), such approximate expression and the exact numerical values for  $\langle p_{\text{intr}}(z) \rangle$  are directly compared. The relation  $\langle p_{\text{intr}}(z) \rangle \approx \sqrt{p_{\text{inc}}}$  indeed yields  $\langle p_{\text{intr}}(z) \rangle \gg p_{\text{inc}}$ , as we expected from the discussion above. Furthermore, this nonlinear relation marks a stark difference with respect to the standard Fabry-Perot interferometer, where a linear relation between incident and intracavity intensities holds [31].

In our model, only for large  $p_{\text{inc}}$  can the average intracavity intensity be well approximated by a linear function of  $p_{\text{inc}}$  [see Fig. 2(a), inset]. Specifically, for large  $p_{\text{inc}}$  the average intracavity intensity asymptotically satisfies the relation  $\langle p_{\text{intr}}(z) \rangle \approx p_{\text{inc}}$ , as expected.

Finally, for low incident power ( $p_{\text{inc}} \lesssim 1$ ), light between the atoms forms a standing wave where nodes are present [see Fig. 2(b), where nodes are at positions  $z = 1/4$  and  $3/4$ ].

It is instructive to show the light intensities at the sites of the TLSs as the distance  $L$  varies, while  $p_{\text{inc}}$  is kept constant. In Figs. 2(c) and 2(d), we plot  $p_1$  and  $p_2$  for incident power  $p_{\text{inc}} = 0.1$  and  $\delta\omega_1 = \delta\omega_2 = 0$ . We notice that at  $L = 0.5$  the light intensity at the TLS1 position is

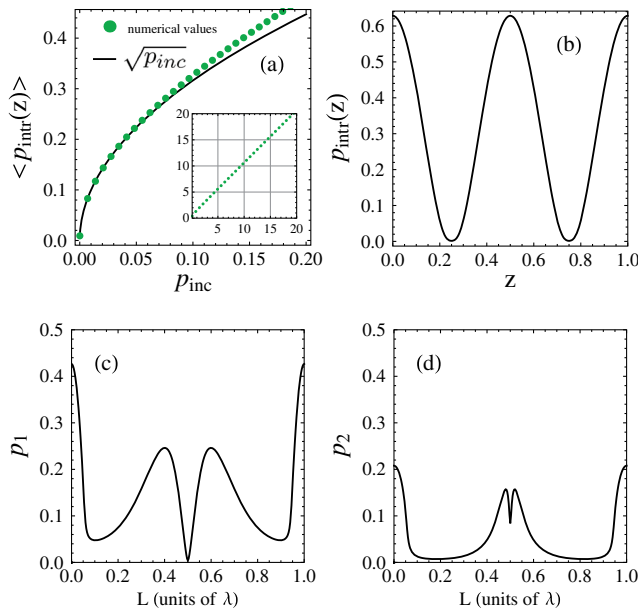


FIG. 2 (color online). (a) Average intracavity intensity. The inset shows the same quantity for larger values of the abscissa. (b) Intracavity intensity. (c) Intensity impinging onto the TLS1. (d) Intensity impinging onto the TLS2.  $p_{\text{inc}}$  is the incident power, while  $L$  is the TLS distance in units of photon wavelength.  $\delta\omega_1 = \delta\omega_2 = 0$  in all panels.  $L = 1$  in (a) and (b).  $p_{\text{inc}} = 0.1$  in (c), and (d).

identically zero and, consequently, the light intensity at the TLS2 position equals the incident intensity. This remains true up to about  $p_{\text{inc}} \lesssim 1$ , and it is caused by the fact that the back reflected light from the TLS2 turns out to be  $\pi$  shifted with respect to the incident light, at the site of the TLS1 (see Ref. [29] for more details).

*Rectification.*—The joint implementation of TLSs and 1D waveguides is believed to represent the future building blocks of nanoscale optoelectronics [32,33]. The realization of nanoscale devices that allow unidirectional light transmission is of utmost importance in this field, and is thus the subject of current research [34,35]. However, most of the attempts to realize or propose optical diodes able to work at the quantum regime lack real miniaturization possibilities and control at the nanoscale [18–20,25–27,36,37]. Here, we show that two TLSs embedded in a 1D waveguide provide the requested features for building a microscopic and integrable optical diode. The realization of this quantum optical diode is feasible with the state-of-the-art technology, as discussed in the following section.

We define the rectifying factor for an optical diode as [20,38]

$$\mathcal{R} = \frac{|T_{12} - T_{21}|}{T_{12} + T_{21}}, \quad (4)$$

where  $T_{12}$  is the transmittance for the case that light is shined from left to right (as in Fig. 1), while  $T_{21}$  is the transmittance in the optical inverse situation where light is shined from right to left. We shall take  $\mathcal{R}$  and  $\mathcal{L} = T_{12}\mathcal{R}$  as figures of merit to quantify the nonreciprocal effects that our microscopic FP interferometer manifests. In Fig. 3, the quantities  $\mathcal{R}$  and  $\mathcal{L}$  are shown as functions of  $L$  and  $\delta\omega_1$ , while  $\delta\omega_2 \approx 0$ . In Figs. 3(a) and 3(b), we investigate the case  $p_{\text{inc}} = 0.001$ , which may be considered equivalent to the single-photon regime (see Fig. S2 of Ref. [29]). High levels of light rectification and transmission are evident. Specifically, some areas in the color scale plot are characterized by both  $\mathcal{R}$  and  $\mathcal{L}$  greater than 0.92. By increasing the incident power, these areas broaden, while  $\mathcal{R}$  and  $\mathcal{L}$  decrease [see Figs. 3(c) and 3(d), where the same quantities are plotted for  $p_{\text{inc}} = 0.1$ ]. In Figs. 3(c) and 3(d), the highest values for  $\mathcal{R}$  is  $\approx 0.53$ , while the highest value for  $\mathcal{L}$  is  $\approx 0.52$ .

High values for  $\mathcal{R}$  and  $\mathcal{L}$  in Figs. 3(a) and 3(b) could be understood as follows. Light is in resonance with the TLS2 and at low power, while it is in general not in resonance with the TLS1, unless we are in the central region of the plots where  $\delta\omega_1 = 0$ . Under such conditions, we have  $R_1 < 1$  and  $R_2 \approx 1$ . When light is incident from right to left, it encounters the TLS2 first, which implies full reflection (being  $R_2 \approx 1$ ). On the other hand, when light is incident from left to right, it encounters the TLS1 first; hence, a significant amount of that light is coherently transmitted to the TLS2 (since  $R_1 < 1$ ). Then, the TLS2 totally reflects such radiation back into the 1D channel to the TLS1. Such

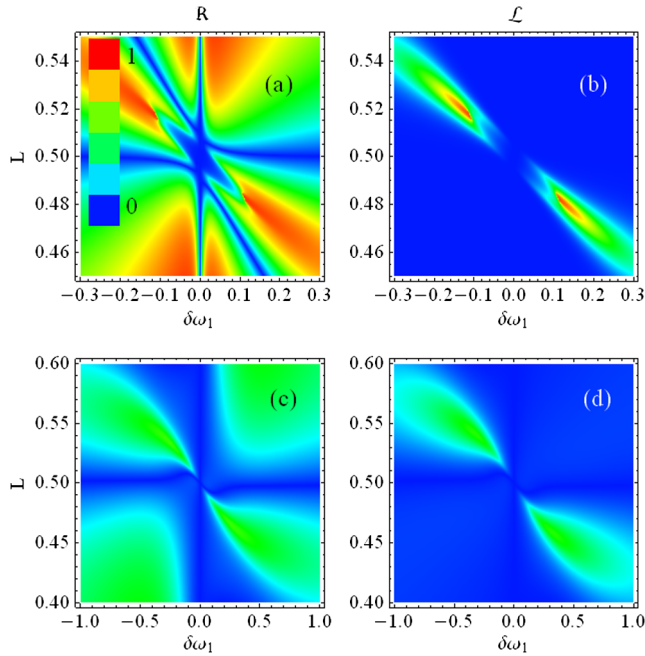


FIG. 3 (color online). Light rectification. Parameters  $\mathcal{R}$  and  $\mathcal{L}$  are plotted.  $\delta\omega_2 = 0$  in all panels.  $p_{\text{inc}} = 0.001$  in (a) and (b).  $p_{\text{inc}} = 0.1$  in (c) and (d).

light acquires a phase shift that depends on  $L$ , due to the path length. At this point, the TLS1 must deal with both the phase-shifted light coming back from the TLS2 and the incident light that is forwardly directed. Both are partially reflected and partially transmitted. However, since light is not in resonance with the TLS1, the light reflected from the TLS1 acquires a phase shift  $\theta_1$  that depends on  $\delta\omega_1$  [see the discussion after Eq. (1)]. The two phase shifts, the one depending on  $L$  and the one depending on  $\delta\omega_1$ , can give constructive or destructive interference. For some values of  $L$  and  $\delta\omega_1$ , we get destructive interference for light exiting the FP interferometer from the left, and constructive interference for light directed toward the TLS2. Those values provide the high level of rectification shown in Fig. 3(a). In Figs. 3(c) and 3(d), both  $R_1$  and  $R_2$  are considerably lower than 1, since here the incident light power is not very low. By reapplying the foregoing discussion, we expect and find a lower degree of light rectification.

We finally point out that the results shown in Fig. 3 do not change significantly within the interval  $-0.01 \lesssim \delta\omega_2 \lesssim 0.01$ . For configurations where none of the two TLSs is in resonance with the incident light beam, there is no region where both  $\mathcal{R}$  and  $\mathcal{L}$  simultaneously display large values.

*Physical implementation.*—The QFP interferometer introduced in this work can be implemented in a number of different technologies and material platforms. In particular, we outline three main architectures as promising candidates to observe such nonreciprocal behavior.

First, superconducting circuits have emerged in the last few years as an outstanding platform to realize quantum

optical functionalities in the microwave range. In this respect, the QFP interferometer can be realized with the state-of-art technology. Considering recent experiments [8], we notice that the system parameters for attaining maximal light rectification and transmission are well within reach. Although it does not represent a miniaturized version of our proposed device, such a microwave circuit implementation of the QFP interferometer is likely to be the most promising candidate for a first proof-of-principle demonstration of the rectifying features, also thanks to the high level of electrostatic control on the state of the single superconducting qubits as TLSs.

As a second alternative, we notice that remarkable progress has been lately achieved in coupling semiconductor quantum dots to 1D photonic wires [12,17] or to semiconducting micropillars [39]. Such artificial atoms behave as almost ideal TLSs, and growing stacks of two or more quantum dots along the same axis and at distances on the order of the optical emission wavelength ( $\sim 1 \mu\text{m}$ ) is at the level of current technology [40]. Moreover, such a nanophotonic platform would naturally represent a fully integrated quantum optical version of our proposed device.

Finally, nitrogen vacancy centers in diamond coupled to 1D surface plasmons [13] can be an interesting possibility to implement a QFP model. In this case, large values of the light-matter coupling rate could be achieved, owing to the strong confinement of plasmonic modes close to the metallic nanowire surface. This could allow us to easily achieve the requested parameter range for light rectification along the 1D axis, i.e., large phase shifts produced by each TLS on incoming light.

The material and engineering efficiency in preparing the 1D system is standardly quantified by an efficiency parameter  $\beta$  ranging from zero (minimal efficiency) to 1 (maximal efficiency).  $\beta$  quantifies the strength of the TLS-light coupling in the 1D material. Remarkably high values of  $\beta$  have been attained in recent experiments: in superconducting circuits  $\beta \approx 0.99$  [8], while in semiconductor quantum dots coupled to photonic wires [41] or to photonic crystals [42]  $\beta \approx 0.95, 0.89$ , respectively.

*Summary and conclusions.*—We modeled a pair of two-level quantum systems embedded in a one-dimensional waveguide as a Fabry-Perot quantum interferometer, where the two quantum systems play the role of highly saturable and nonlinear mirrors. Beside manifesting nonlinear effects, this quantum interferometer can work as a very efficient integrated optical diode, with unprecedented figures of merit in terms of simultaneous light rectification and transmission, and thus with potential applications in integrated optical photonics. Such a quantum optical diode can be implemented with several integrated one-dimensional designs employing different state-of-the-art technologies and materials, and dimensions ranging from nanometer to millimeter sizes. Unconditional quantum rectification (i.e., rectification of quantum states) is the ultimate goal of this research field,

and has not yet been realized. We here suggest that the present system could be investigated in the fully quantum regime (considering quantum states for the input light field) as a strong candidate for photonic rectification.

F. F., E. M., D. V., and M. F. S. acknowledge financial support from Conselho Nacional de Desenvolvimento Científico e Tecnológico (CNPq). D. V. acknowledges support from CNPq, through the Chamada Universal No. 477612/2013-0. A. A. and J.-P. P. acknowledge support from Agence National de la Recherche (WIFO project). D. G. acknowledges the Italian Ministry of University and Research (MIUR) through FIRB—Futuro in Ricerca Project No. RBFR12RPD1, and CNPq through the PVE/CSF Project No. 407167/2013-7. L. S. and F. F. acknowledges partial support by the Research Council for Natural Sciences and Engineering of the Academy of Finland. L. S. acknowledges financial support from the Marie Curie Actions (Marie Curie Actions) of the European Union's Seventh Framework Programme (FP7/2007-2013) under REA Grant Agreement No. [291734].

\*ffratini@fisica.ufmg.br; fratini.filippo@gmail.com

- [1] J. T. Shen and S. Fan, *Opt. Lett.* **30**, 2001 (2005); *Phys. Rev. Lett.* **98**, 153003 (2007).
- [2] D. E. Chang, A. S. Sorensen, E. A. Demler, and M. D. Lukin, *Nat. Phys.* **3**, 807 (2007).
- [3] J. T. Shen and S. Fan, *Phys. Rev. Lett.* **98**, 153003 (2007).
- [4] D. Valente, Y. Li, J. P. Poizat, J. M. Gérard, L. C. Kwek, M. F. Santos, and A. Auffèves, *Phys. Rev. A* **86**, 022333 (2012).
- [5] G. Hétet, L. Slodička, M. Hennrich, and R. Blatt, *Phys. Rev. Lett.* **107**, 133002 (2011).
- [6] C. Monroe and J. Kim, *Science* **339**, 1164 (2013).
- [7] A. A. Abdumalikov, Jr., O. Astafiev, A. M. Zagoskin, Yu. A. Pashkin, Y. Nakamura, and J. S. Tsai, *Phys. Rev. Lett.* **104**, 193601 (2010).
- [8] A. F. van Loo, A. Fedorov, K. Lalumière, B. C. Sanders, A. Blais, and A. Wallraff, *Science* **342**, 1494 (2013).
- [9] K. Lalumière, B. C. Sanders, A. F. van Loo, A. Fedorov, A. Wallraff, and A. Blais, *Phys. Rev. A* **88**, 043806 (2013).
- [10] I. Yeo, P.-L. de Assis, A. Gloppe, E. Dupont-Ferrier, P. Verlot, N. S. Malik, E. Dupuy, J. Claudon, J.-M. Gérard, A. Auffèves, G. Nogues, S. Seidelin, J.-Ph. Poizat, O. Arcizet, and M. Richard, *Nat. Nanotechnol.* **9**, 106 (2014).
- [11] A. V. Akimov, A. Mukherjee, C. L. Yu, D. E. Chang, A. S. Zibrov, P. R. Hemmer, H. Park, and M. D. Lukin, *Nature (London)* **450**, 402 (2007).
- [12] T. Lund-Hansen, S. Stobbe, B. Julsgaard, H. Thyrrstrup, T. Sünner, M. Kamp, A. Forchel, and P. Lodahl, *Phys. Rev. Lett.* **101**, 113903 (2008).
- [13] A. Huck, S. Kumar, A. Shakoor, and U. L. Andersen, *Phys. Rev. Lett.* **106**, 096801 (2011).
- [14] R. C. Ashoori, *Nature (London)* **379**, 413 (1996).
- [15] D. R. Stewart, D. Sprinzak, C. M. Marcus, C. I. Duruöz, and J. S. Harris, Jr., *Science* **278**, 1784 (1997).
- [16] P. M. McEuen, *Science* **278**, 1729 (1997).
- [17] J. Claudon, J. Bleuse, N. S. Malik, M. Bazin, P. Jaffrennou, N. Gregersen, C. Sauvan, P. Lalanne, and J.-M. Gérard, *Nat. Photonics* **4**, 174 (2010).
- [18] D. Roy, *Phys. Rev. B* **81**, 155117 (2010).
- [19] Y. Shen, M. Bradford, and J. T. Shen, *Phys. Rev. Lett.* **107**, 173902 (2011).
- [20] E. Mascarenhas, D. Gerace, D. Valente, S. Montangero, A. Auffèves, and M. F. Santos, *Europhys. Lett.* **106**, 54003 (2014).
- [21] D. Gerace, H. E. Türeci, A. Imamoğlu, V. Giovannetti, and R. Fazio, *Nat. Phys.* **5**, 281 (2009).
- [22] F. Kien, S. Dutta Gupta, K. P. Nayak, and K. Hakuta, *Phys. Rev. A* **72**, 063815 (2005).
- [23] C. A. Büsser and F. Heidrich-Meisner, *Phys. Rev. Lett.* **111**, 246807 (2013).
- [24] H. Zheng and H. U. Baranger, *Phys. Rev. Lett.* **110**, 113601 (2013).
- [25] Z. Yu, G. Veronis, Z. Wang, and S. Fan, *Phys. Rev. Lett.* **100**, 023902 (2008).
- [26] C. Mu-Tian, *Commun. Theor. Phys.* **58**, 151 (2012).
- [27] H. Lira, Z. Yu, S. Fan, and M. Lipson, *Phys. Rev. Lett.* **109**, 033901 (2012).
- [28] D. Valente, S. Portolan, G. Nogues, J. P. Poizat, M. Richard, J. M. Gérard, M. F. Santos, and A. Auffèves, *Phys. Rev. A* **85**, 023811 (2012).
- [29] See Supplemental Material at <http://link.aps.org/supplemental/10.1103/PhysRevLett.113.243601> for the details on a) the derivation of the reflectances of the TLSs, b) the derivation of the equations used for the Fabry Perot Model, c) the analysis on the phase shifted light reflected by the TLS2, which guarantees zero field at the location of the TLS1, d) validation of our semiclassical model by comparing with full quantum mechanical models., which includes Ref. [30].
- [30] D. Valente, Ph.D. thesis, University of Grenoble, Néel Institute CNRS, 2012. Available online at <https://tel.archives-ouvertes.fr/tel-00859710>.
- [31] A. Yariv and P. Yeh, *Photonics, Optical Electronics in Modern Communications*, 6th ed. (Oxford University Press, New York, 2007), Chap. 4.
- [32] X. Duan, *Nature (London)* **409**, 66 (2001).
- [33] S. Coe-Sullivan, *Nat. Photonics* **3**, 315 (2009).
- [34] L. Bi, J. Hu, P. Jiang, D. Hun Kim, G. F. Dionne, L. C. Kimerling, and C. A. Ross, *Nat. Photonics* **5**, 758 (2011).
- [35] L. Fan, J. Wang, L. T. Varghese, H. Shen, B. Niu, Y. Xuan, A. M. Weiner, and M. Qi, *Science* **335**, 447 (2012).
- [36] M.-T. Cheng, X.-S. Ma, M.-T. Ding, Y.-Q. Luo, and G.-X. Zhao, *Phys. Rev. A* **85**, 053840 (2012).
- [37] D.-W. Wang, H.-T. Zhou, M.-J. Guo, J.-X. Zhang, J. Evers, and S.-Y. Zhu, *Phys. Rev. Lett.* **110**, 093901 (2013).
- [38] S. Lepri and G. Casati, *Phys. Rev. Lett.* **106**, 164101 (2011).
- [39] V. Loo, C. Arnold, O. Gazzano, A. Lemaitre, I. Sagnes, O. Krebs, P. Voisin, P. Senellart, and L. Lanco, *Phys. Rev. Lett.* **109**, 166806 (2012).
- [40] A. Badolato, K. Hennessy, M. Atatüre, J. Dreiser, E. Hu, P. M. Petroff, and A. Imamoğlu, *Science* **308**, 1158 (2005).
- [41] M. Munsch, N. S. Malik, E. Dupuy, A. Delga, J. Bleuse, J.-Michel Gérard, J. Claudon, N. Gregersen, and J. Mørk, *Phys. Rev. Lett.* **110**, 177402 (2013); **111**, 239902(E) (2013).
- [42] T. Lund-Hansen, S. Stobbe, B. Julsgaard, H. Thyrrstrup, T. Sünner, M. Kamp, A. Forchel, and P. Lodahl, *Phys. Rev. Lett.* **101**, 113903 (2008).